# Effective stiffness method for rigid monopile foundations of offshore wind turbines and in-situ validation

Versteijlen, Pim; Renting, Frank; Valk, van der, P.L.C.; Bongers, J.; van Dalen, Karel; Metrikine, Andrei

**DOI**
10.1016/j.proeng.2017.09.349

**Publication date**
2017

**Document Version**
Final published version

**Published in**
Procedia Engineering

**Citation (APA)**
Versteijlen, P., Renting, F., Valk, van der, P. L. C., Bongers, J., van Dalen, K., & Metrikine, A. (2017). Effective stiffness method for rigid monopile foundations of offshore wind turbines and in-situ validation. *Procedia Engineering*, *199*, 3248–3253. https://doi.org/10.1016/j.proeng.2017.09.349

Available online at www.sciencedirect.com

ScienceDirect

Procedia Engineering 199 (2017) 3248–3253

Procedia Engineering

www.elsevier.com/locate/procedia

X International Conference on Structural Dynamics, EURODYN 2017

# Effective stiffness method for rigid monopile foundations of offshore wind turbines and in-situ validation

W.G. Versteijlen[a,b], F.W. Renting[b], P.L.C. van der Valk[a], J. Bongers[a], K.N. van Dalen[b], A.V. Metrikine[b]

[a] *Siemens Wind Power, Beatrixlaan 800, 2595 BN Den Haag, The Netherlands*
[b] *Faculty of Civil Engineering and Geosciences, Delft University of Technology, Stevinweg 1, 2628CN Delft, The Netherlands*

**Abstract**

It is widely accepted that the initial stiffness derived with the *p-y* methodology as prescribed by the American Petroleum Institute does not capture the true small-strain stiffness for rigidly behaving piles. We present an alternative method, capturing the 3D effects in the soil-pile interaction, in which the soil is characterized with in-situ seismic measurements. As the design of the foundations of offshore wind turbines often involves many expensive load simulations (load cases), the method also includes finding an effective 1D or Winkler stiffness yielding a similar pile response as in the 3D model. The method is exemplified for a real 5 m-diameter monopile embedded in stiff dense sand, in a near-shore wind farm in The Netherlands. The dynamic properties of this pile have been tested (prior to installation of the super-structure) with a unique measurement setup using a hydraulic shaker, exciting between 1 and 9 Hz. The response of this stand-alone pile is highly sensitive to the soil and allowed us to verify the effective 1D stiffness with much higher certainty as opposed to the usual situation including dynamic disturbances and uncertainties related to the interaction with the super-structure. The effective soil damping of the pile is estimated, and the performance of both the standard design (*p-y*) stiffness method and the proposed effective stiffness method is assessed in view of the measured strains and accelerations.


Peer-review under responsibility of the organizing committee of EURODYN 2017.

*Keywords:* Effective soil stiffness; rigid piles; offshore wind foundations; in-situ shaker testing; resonance; soil damping

## 1. Introduction

One of the large cost-saving potentials to make offshore wind economically more competitive, is increased understanding of the soil-structure interaction (SSI) occurring at the most often applied monopile (MP) foundation. Due to uncertainty in this field of expertise, it is expected that too much conservatism is applied in design, leading to over-designed piles. The issue with many of the developed SSI models and methods [1] - [3] is that these were aimed at and calibrated for the lateral behaviour of long flexible behaving piles, whereas the mostly applied monopile foun-

* Corresponding author.
*E-mail address:* pim.versteijlen@siemens.com

1877-7058 
Peer-review under responsibility of the organizing committee of EURODYN 2017.
10.1016/j.proeng.2017.09.349

dation for offshore wind turbines (OWTs) is a rigidly behaving structure. The soil reaction is fundamentally different for these cases (flexible and rigid behaving piles). Another issue is that so far no validation studies are available of real-sized, in-situ MPs being horizontally excited in a dynamic way (in line with the vibrations expected offshore). Over the past few years we developed a method to predict the SSI stiffness, based on small-strain, seismic soil characterization and 3D modelling [4], and also developed a useful technique to translate the 3D results into useable 1D effective models [5]. We have now closed this research loop by performing 'first-off' in-situ validation measurements on an installed MP, using a hydraulic shaker to excite the structure with a known force input. In this paper we give a concise explanation of the performed tests and we assess how well the 1D effective stiffness method performs in predicting the in-situ stiffness. This paper is based on [6], in which a more elaborate rendition of the content is given.

## 2. Predicted in-situ effective stiffness

The soil profile at position 'W27', where the shaker excitation tests were performed, can be characterized to consist of mostly medium dense to dense sand, with a thin clay or peat layer near the top and another thin clay layer near the tip of the pile. An extensive amount of in-situ soil characterization testing has been performed at this location. In this paper we will use the output of the conventional CPT and laboratory testing on borehole samples and the seismic CPT (SCPT). The upper left three panels of Figure 1 show the profiles of the density $\rho(z)$, the Young's modulus $E(z)$ and Poisson's ratio $\nu(z)$ of the location. The density (submerged unit weight) was derived from laboratory tests, and the Poisson's ratio $\nu$ was estimated based on the (saturated) soil type; 0.25 for sand, 0.4 for clay and 0.43 for peat. Determining a precise value for $\nu$ is challenging, however, the pile displacement is not very sensitive to this parameter, as long as $\nu$ is well below the incompressibility limit of 0.5 [5]. The shear modulus $G$ and Young's modulus are calculated with their relation to the estimated shear wave velocity $c = \sqrt{E/2(1+\nu)\rho} = \sqrt{G/\rho}$, which in turn was found with the SCPT time traces, using a previously explained technique [5]. These profiles (upper left 3 panels, Figure 1) were used as input for a linear elastic 3D finite element soil-pile model, in which a 1 m homogeneous layer thickness was assumed for the stratified soil. The model was developed using ANSYS software, choosing solid elements for the soil that are fully attached to the shell elements of the pile. The linear elastic simplification of the soil was ascertained to be justified for the occurring displacements of the pile during shaker excitation by assessing the force-displacement relations and an investigation into the probable soil strains [6]. In general it is believed that installed OWT foundation-soil systems operate mostly in the linear elastic strain regime of the soil [7]. From the static response of the 3D pile (in terms of displacements and rotations) we calculated a 1D effective Winkler stiffness profile $k_{eff}(z)$, using a previously developed technique [5]. The resulting distributed stiffness profile is presented in the upper right panel of Figure 1, in which, as a reference, also a 'best-estimate' (unconservative) *p-y* curve initial stiffness is given. Note that the horizontal axis has a logarithmic scale. We would like to emphasize that this $k_{eff}(z)$ is truly a SSI parameter; it captures the properties of both the soil and the pile. Since the pile is in this case rather rigid, causing more global soil reactions, $k_{eff}(z)$ does not directly reflect the local properties of the soil. Clearly this is more the case for the *p-y* curve profile; being calibrated for flexible piles, assuming local soil reactions, it reflects the locality of the weak layers at the top of the profile and at around 20 m depths. Using $k_{eff}(z)$ to model a 1D Timoshenko beam on Winkler foundation, and applying the same loading as in the 3D model, we retrieved the match with the 3D model in terms of displacement, slope, rotation and curvature as presented in the lower four panels of Figure 1. Again, as a reference, also the response of the beam supported by the initial stiffness profile derived by the *p-y* curve method are presented in these panels. In Section 4, $k_{eff}(z)$ will be used as an initial guess stiffness profile to model (match) the in-situ measured response.

## 3. Performed tests

Prior to installation, pile W27 was equipped with 7 rings of 4 strain gauges (placed along the four quadrants) on the inside wall of the MP, see the left panel of Figure 2. In addition, during shaker excitation, 2 accelerometers were connected to the pile head, and one accelerometer was placed on the shaker frame. Furthermore, 16 sets of accelerometers and piezometers were placed in the vicinity of the pile in the soil, in an attempt to truly capture the soil-structure interaction. Nevertheless, in this paper we will only analyze the output of the pile sensors: strain gauges and accelerometers. During the limited available testing time offshore, we performed three tests, each having different

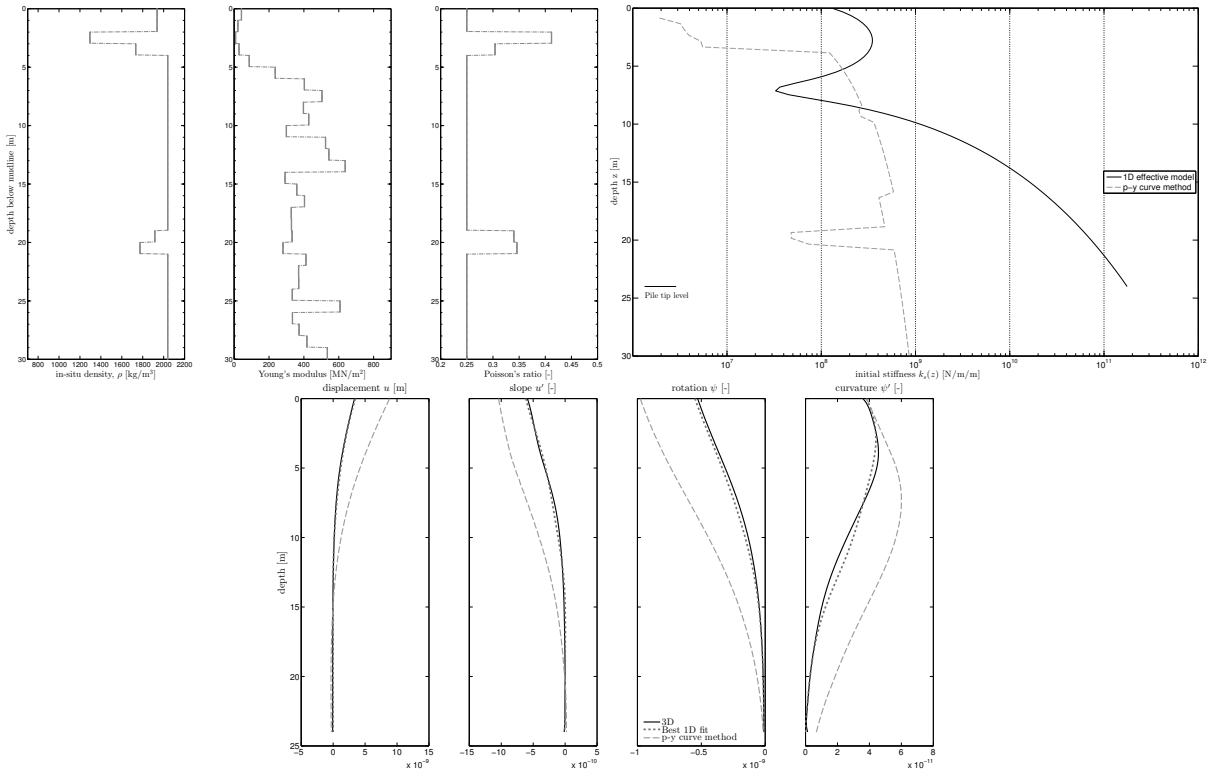


Figure 1. Upper left panels, from left to right: in-situ $\rho(z)$, $E(z)$ and $\nu(z)$. Upper right panel: the effective $k_{eff}(z)$ (black solid line). This initial stiffness incorporates 3D modelling effects and small-strain elastic properties of the soil obtained using in-situ seismic measurements. The *p-y* curve initial stiffness is given by the grey dashed line. Lower four panels, from left to right: the displacement, slope, rotation and curvature of a Timoshenko beam supported by the effective Winkler profile $k_{eff}(z)$ (dark grey dotted line) and by the *p-y* curve initial stiffness profile (light grey dashed line) compared with the original 3D linear elastic model. To obtain an equivalent bending shape as induced by the shaker, a horizontal force of 1 N and overturning moment of 9.85 Nm was applied to the head of the 3D pile model.

ballast weights placed on the rotating cogwheels of the hydraulic shaker. The frequency of excitation varied between 1.04 and 8.68 Hz, and the 'arm ($R$) x weight ($m$)' was calibrated [8] for the shaker to be 239.32 mkg for the Heavy weight setup, 88.76 and 32.08 mkg for the Middle and Light weight setups, respectively. These numbers can be used to compute the centrifugal force amplitude: $F = m\omega^2 R$. with $\omega$ the angular frequency. We will focus on the stepped-sine frequency sweeps that were performed; steady-state signals were retrieved for strain gauge rings 2-7 (the lowest ring failed during pile installation) and the accelerometers on the pile and shaker. Time windows of constant-frequency excitation were selected and the signals were low-pass filtered to identify the steady-state amplitudes of the measured strains and accelerations.

## 4. Identified in-situ stiffness

In this section, the measured response is compared to the predicted (modelled) response. To this end, we use the previously presented stiffness profile $k_{eff}(z)$ as an initial guess for the Winkler foundation in a dynamic Timoshenko model (see left panel of Figure 3; for brevity, the common governing equations are not given in this paper). The soil damping profile $c(z)$ is assumed to have the same shape as the stiffness profile: $c(z) = \alpha \cdot k_{eff}(z)$, with $\alpha$ a damping coefficient that will be tuned according to the measured transfer functions. For each steady-state frequency $f$ and weight setup, the modelled (frequency domain) response in terms of internal transmissibility amplitudes are compared to those calculated for the in-situ recordings. The amplitude of the transmissibility function is defined as the ratio between the axial strain amplitude $\epsilon_i$ of the pile at various heights ($i = 2..7$ for strain gauge rings 2 to 7, the left panel of Figure 2) and the displacement amplitude of the pile head $u_p$, which is retrieved by dividing the pile head accelerations $A_p$ by $\omega^2$, see Equation 1. It was found that applying the calibrated shaker force amplitude $F$, or


Figure 2. Left panel: measurement setup for pile W27. The orange boxes indicate the positions of the cones equipped with accelerometers and pore water pressure meters. The hatched spots on the pile (named A-D-C) indicate the position of the strain gauges, with their ring number indicated at the left side of the pile. A borehole classification of the soil is given in the right side of the figure, with yellow indicating sand, green for clay and brown for peat. Right panel: aerial photo showing the shaker on pile W27, the mobilized barges and crane.

the recorded acceleration amplitude as recorded on the shaker, did not yield equal modelled response. Assessing the transmissibility instead of directly the strains and accelerations, evades any errors made in determining the exact forcing of the pile. We investigate what stiffness factor $\gamma$ is needed for a best match in modelled and measured response; what $\gamma$ minimizes the difference in transmissibility, see Equation 2.

$$T_i(f) = \frac{\epsilon_i(f)}{u_p(f)} = \frac{\epsilon_i(f)\omega^2}{A_p(f)} \tag{1}$$

$$\min_{\gamma} \left| \left( \frac{\sum_{i=2}^{i=7} |T_i - \overline{T}_{(\gamma)i}|^2}{\sum_{i=2}^{i=7} |T_i|^2} \right)^{\frac{1}{2}} \right| \tag{2}$$

The overlined symbols in Equation 2 indicates that this is the corresponding modeled quantity. In this optimization, we thus do not change the shape of $k_{eff}(z)$; merely a single factor is applied to increase or decrease the stiffness. The left panel of Figure 4 shows the different factors $\gamma$ that give the best match between modelled and measured transmissibility. A frequency-dependency of the stiffness is apparent: $\gamma(f)$. A softening seems to occur with increasing frequency up to 5 - 6 Hz, after which a stiffening seems to take place. We investigated whether the softening of the stiffness with frequency could be related to the mobilization of added mass. When modelling extra inertia, indeed $\gamma$ turns out to be less frequency-dependent (constant stiffness up to 5 - 6 Hz). The observed stiffening for the higher frequencies could be related to undrained behaviour of the saturated sand. The $\gamma$ for the lowest frequency of around 1 Hz is of most relevance for OWTs. It is expected that the same stiffness applies for the typically low natural frequencies of OWTs (±0.3 Hz). Our stiffness estimation method seems to over-predict this stiffness by about 20%; a factor of about $\gamma = 0.8$ needs to be applied to match the in-situ stiffness. Figure 3 show an example fit of the measured and modelled strains (middle panel) and displacements (right panel) for the Heavy weight setup at 1.045 Hz excitation frequency. In these figures the previously discussed discrepancy can be observed between using either a force-controlled or an acceleration controlled model. To compare the performance of our effective stiffness method with the design approach, we calculated the $\gamma(f)$ for the best-estimate *p-y* curve initial stiffness (upper right panel Figure 1); these are given in the right panel of Figure 4. A $\gamma$ of around 2.4 seems to be applicable for the low-frequency stiffness: an underestimation of the occurring stiffness with 140% by the *p-y* curve method. The variability in $\gamma(f)$ is somewhat larger for the *p-y* curve profile. This could be caused by a larger mismatch in the shape of the *p-y* stiffness profile and the in-situ profile, and the fact that the stiffness is lower (than the effective stiffness).

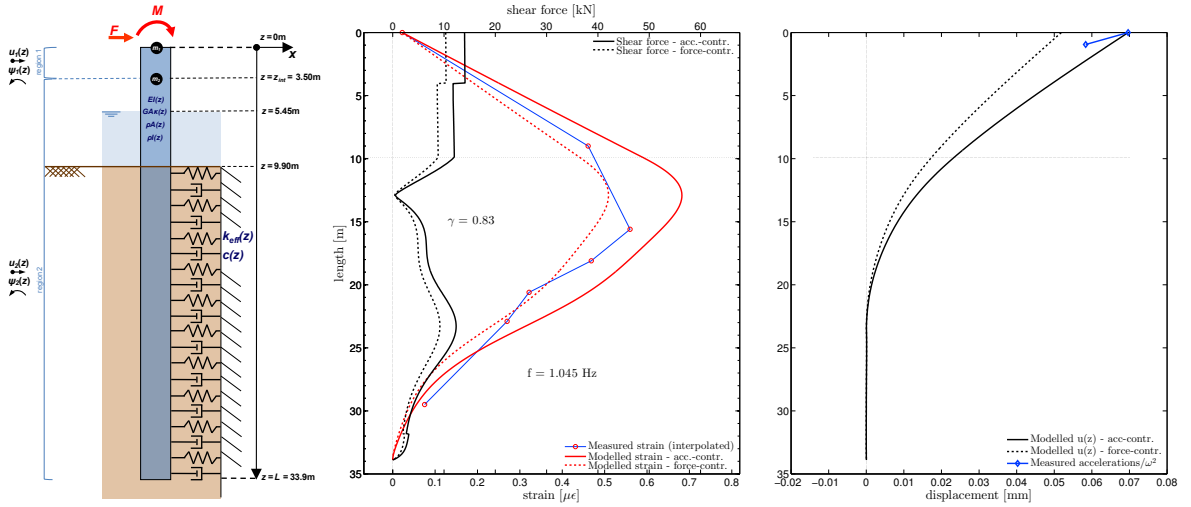


Figure 3. Left panel: graphical representation of the basic 1D model, the used reference frame and sign conventions. Middle and right panels: match in strains with a stiffness correction factor $\gamma$ retrieved by optimizing for the internal transmissibility (left panel Figure 4), for the Heavy weight setup, excitation frequency of 1.045 Hz. The absolute values of both the acceleration- and force-controlled modelled responses are shown in terms of shear force and strain (middle panel) and displacements (right panel).

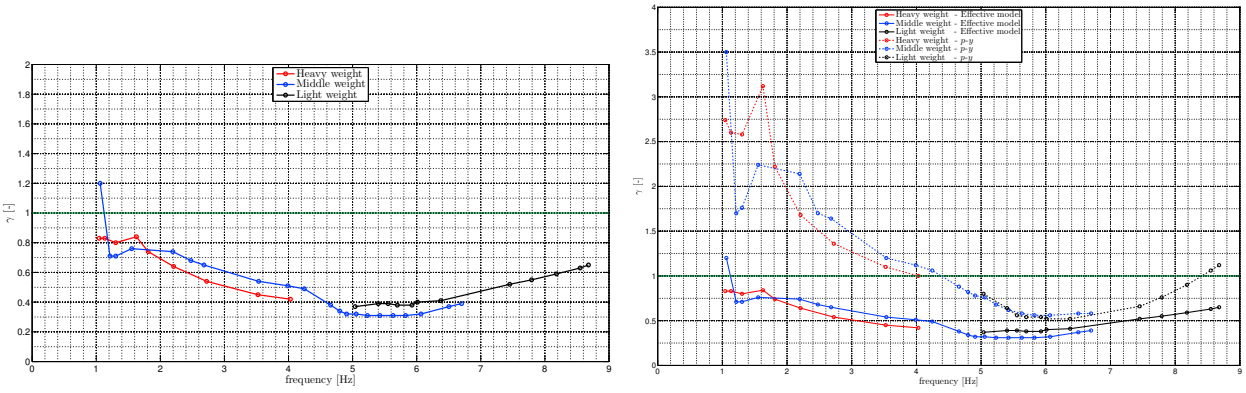


Figure 4. Left panel: stiffness correction factors $\gamma$ applied to the effective 1D stiffness profile (as presented in Section 2) to minimize the mismatch between modeled and measured transmissibilities $T$ (Equation 2) of the 3 weight setups. The first point of the of the Middle weight setup (blue line) is considered to be an outlier. Right panel: factors $\gamma$ found by optimizing the $p$-$y$ initial stiffness profile to match the measured transmissibility function $T$. The $\gamma(f)$ for the effective stiffness profile are again shown to serve as a reference.

As the Middle weight setup covers the widest frequency band, we will focus a bit more on that test. When applying the frequency-dependent stiffness $\gamma(f)$ on $k_{eff}(z)$ as given by Figure 4, we retrieve the match in transmissibility and transfer functions as given in respectively the left and right panel of Figure 5. The transfer functions are defined as $H_i(f) = \frac{\epsilon_i(f)}{F(f)}$. The transfer functions allow us to tune the damping coefficients; $c(z) = \alpha \cdot k_{eff}(z)$, with $\alpha = 2.08 \cdot 10^{-2}$ s for the match shown in the right panel of Figure 5. Using the obtained damping coefficients and a mean stiffness correction factor $\gamma$ of the frequencies around resonance to simulate the response, we extracted the damping contribution of the soil with the half-power bandwidth method, yielding a critical damping ratio of $\zeta = 20\%$ for this stand-alone MP. This is a high damping indeed, however note that the relative contribution to the damping of the extended full structure (tower and turbine) will be much smaller; assuming frequency-independent damping, the observed soil damping is estimated to contribute a 0.14% critical damping for the full OWT structure. This value is in agreement with that identified using the current monitoring program of the full structure. Other than for the MP-only damping, this is a rather low damping value, which could be related to the stiff character of the soil profile, leading to small displacements.

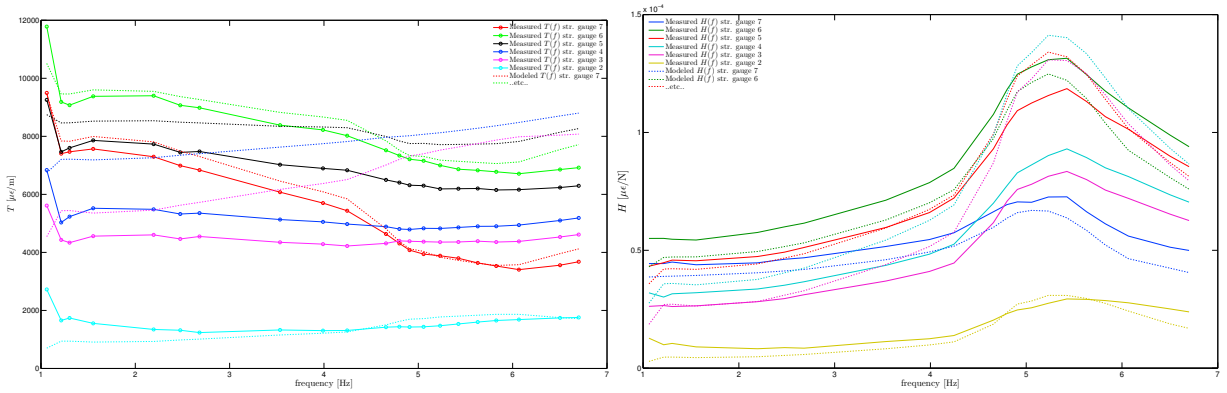


Figure 5. Measured (continuous lines) and modeled (dotted lines) transmissibility (left panel, Equation 1) and transfer (right panel) functions of the strain gauges for the Middle weight setup.

## 5. Discussion & conclusions

In this contribution, we gave a brief insight into the 'first-off' in-situ, real-sized monopile testing we performed. We used a hydraulic shaker to excite the structure, and recorded the sub-soil strains of the pile and the accelerations and pore water pressures in the near-field soil. A short assessment was presented in which the stiffness profile rendered by our 1D effective stiffness method is compared to the apparent in-situ stiffness, and additionally to the best-estimate *p-y* curve profile prescribed by design standards. Where the 1D effective stiffness method seems to over-estimate the in-situ stiffness with 20%, the *p-y* curve initial stiffness profile under-estimates the in-situ stiffness with 140%. Given the opportunities to further improve the developed method, these validation measurements have further improved our confidence in the method: a combination of in-situ seismic measurements, 3D modelling and 3D-1D translation. We would like to refer the interested reader to [6] for more details on this work.

## Acknowledgements

The work is part of the DISSTINCT project [9] [10], which is partly funded by the Dutch government (proj. no. TKIWO2001). We would also like to thank Westermeerwind (the owner of the wind farm) and Van Oord (foundation designer and installation contractor) for their cooperation, Robin Greeuw for his valuable contribution in calibrating the shaker, and Hendrik Kramers for his full OWT identifcation analyses.

## References

[1] G. Gazetas, R. Dobry, Horizontal Response of Piles in Layered Soils, J. Geotech. Eng. 110 (1984) 20–40.
[2] M. Novak, T. Nogami, Soil-pile interaction in horizontal vibration, Earthquake Engineering & Structural Dynamics 5 (1977) 263–281.
[3] L. M. Kagawa, Takaaki and Kraft, Dynamic characteristics of lateral load-deflection relationships of flexible piles, Earthq. Eng. Struct. Dyn. 9 (1981) 53–68.
[4] W. G. Versteijlen, K. N. van Dalen, A. V. Metrikine, L. Hamre, Assessing the small-strain soil stiffness for offshore wind turbines based on in situ seismic measurements, in: J. Phys. Conf. Ser., volume 524, IOP Publishing, 2014, p. 012088. doi:10.1088/1742-6596/524/1/012088.
[5] W. G. Versteijlen, A. V. Metrikine, K. N. van Dalen, A method for identification of an effective winkler foundation for large-diameter offshore wind turbine support structures based on in-situ measured small-strain soil response and 3D modelling, Engineering Structures 124 (2016) 221–236.
[6] W. G. Versteijlen, F. W. Renting, P. L. C. van der Valk, J. Bongers, K. N. van Dalen, A. V. Metrikine, Effective soil-stiffness validation: Shaker excitation of an in-situ monopile foundation, Soil Dyn Earthq Eng *Under review* (2017).
[7] M. Damgaard, V. Zania, L. V. Andersen, L. B. Ibsen, Effects of soil-structure interaction on real time dynamic response of offshore wind turbines on monopiles, Engineering Structures 75 (2014) 388–401.
[8] R. Greeuw, Preliminary analysis of experimental data in offshore shaker tests, Technical Report, Delft University of Technology, 2016. Internship report.
[9] W. G. Versteijlen, S. N. Voormeeren, Efficient support structure design through improved dynamic soil structure interaction modeling, Technical Report, 2013. TKI-WoZ Project Description, DISSTINCT.
[10] TKI Wind op Zee DSSI project (DISSTINCT), http://tki-windopzee.nl/project/dssi, ???? Accessed: 2016-08-10.